Dust Figure Guided Modeling of Corona Discharge on Touchscreen Surface

Zhekun Peng
EMC Laboratory
Missouri University of Science and Technology
Rolla, MO, USA
pengzhe@mst.edu

Jianchi Zhou
Apple Inc.
Cupertino, CA, USA
jianchi_zhou@apple.com

Darryl Kostka
Apple Inc.
Cupertino, CA, USA
dkostka@apple.com

David Pommerenke
Institute of Electronics Graz University of Technology & SAL Graz EMC lab
Graz, Austria
david.pommerenke@tugraz.at

Daryl Beetner
EMC Laboratory
Missouri University of Science and Technology
Rolla, MO, USA
daryl@mst.edu

***Abstract*—Electrostatic discharge to a touchscreen display leads to a corona discharge which creates corona streamers that propagate along the glass surface. The streamers couple energy to touch sensors underneath the glass which may then cause failure. Modeling the ionized air resistance and the current distribution on the glass surface from corona discharge is challenging. A new methodology is proposed for modeling corona discharge to a touchscreen surface with the help of experimentally measured dust figures. A geometric analysis of the dust figure and how streamer currents couple to the sensor patch matrix is given to explain the modeling method. A SPICE model is proposed to better correlate the ESD gun current with the current coupled to the sensor patches. The ability of the model to predict peak current, charge and rise time is evaluated. Predictions of peak current and charge are within 30% error.**

Keywords—Dust Figure, Electrostatic Discharge, Air Discharge, Corona Discharge, Touchscreen, Streamer Propagation

I. Introduction

Electrostatic Discharge (ESD) may cause unintentional disruption of electronic devices. A human handling a portable device can cause an ESD discharge to the touchscreen of the device when touching it with fingertips or metallic items [1]. Because of the high impedance and dielectric breakdown strength of glass, the discharge does not cause a spark but creates an ionized corona which flows across the surface of the screen. As the charge flows across the glass surface, significant energy can be coupled, mainly via displacement current, to the sensors and chips under the screen, which can cause soft and hard failures in the device [2]. Combined with ESD protection models for the IC and system [3], models for the corona discharge to the touchscreen could allow designers to evaluate system-level ESD robustness at the pre-compliance level.

IEC 61000-4-2 defines ESD air discharge test methods for insulating surfaces [4]. When the round tip of an ESD gun approaches the glass surface of a touchscreen, the air is ionized between the tip and glass surface after the electric field strength passes a threshold [5, 6]. The ionized air creates a region of conductive plasma [7]. The strong tangential E-field created by the ESD gun drives the expansion of the ionized area. Displacement current from the ionized air to patches under the glass allows energy to be coupled to the touchscreen circuity. The parameters of patch circuitry include the surface to patch capacitance (glass capacitance according to patch size), patch to return path capacitance, and indium-tin-oxide (ITO) trace resistance [2]. An example of a corona discharge above touchscreen sensor patches and the patch circuitry are shown in Fig. 1.

This work was supported in part by the National Science Foundation (NSF) under Grant IIP-1916535.

Previous studies of corona discharge to touchscreen surfaces purely focused on either discharge current or patch current. A. Talebzadeh *et al* [8] focused on the current through the ESD gun. S. Shinde *et al* [9] studied the current coupled to the sensors with a substitution PCB. Y. Gan *et al* [1] studied how the displacement current into adjacent sensor patches changes as the charge flows across the glass surface. These studies, however, did not correlate the current into the sensor patches with the ionized air on the glass surface. An attempt to estimate an equivalent source for the glass discharge current was made using a genetic algorithm [10] but the method requires an experimental waveform of the current coupled through the sensor patch to be available and the equivalent source is not valid for different PCB setups or glass thicknesses.

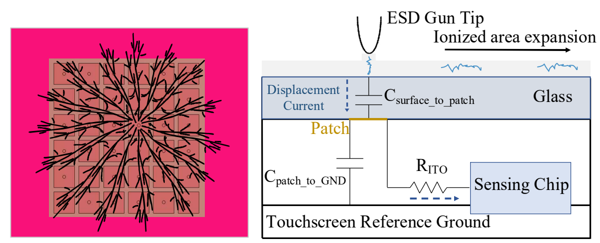

Fig. 1. Depiction of a corona discharge to a touchscreen surface with sensor patch matrix beneath (left) and patch circuitry (right).

The Lichtenburg dust figure method is commonly used to visualize the invisible charge distribution left after a corona surface discharge [11, 12, 13, 14]. Many studies of surface discharge on insulators utilize the dust figure method to analyze how the figures change with factors such as pulse duration [15], voltage level, polarity [16] and humidity [17]. Dust figures have been applied to corona discharge to touchscreens to investigate how dust figure size and shape change with discharge levels, polarity, discharge modes [1] and glass types [18]. None of these studies correlate the propagating corona streamers with the current waveform. Full-wave simulation models in [18] demonstrate that the discharge current can be estimated by treating the surface discharge as a resistive disk where conductivity reduces inversely with the disk radius, but no analysis to the patch current or physical explanation for this result was available.

In this paper, observations of experimental dust figures are used to develop a model for corona surface currents and associated displacement current into sensor patches. This analysis helps to explain previous models treating the surface discharge as a resistive disk with varying conductivity. The resulting model is used to predict the current through the ESD gun and coupling to the touchscreen sensor patches. Peak current, charge and rise time are compared between the model and the measurement.

II. Dust Figure Measurement

Fig. 2 illustrates the propagation of a corona discharge streamer on a touchscreen. When a certain electric field strength is reached between the ESD gun tip and the glass (about 3 kV/mm [19]), the air between the gun tip and the glass is ionized, causing the air to become conductive. The level of conductivity depends on the number of free carriers (e.g. ions) in the channel [16], which will change over the course of the discharge. As current flows from the ESD gun through the ionized air, displacement current flows through the glass to the patch and a high E-field is created tangential to the glass surface at the end of each streamer. The high E-field allows the ionized region to expand until the E-field at the edges is too low to sufficiently ionize the surrounding air.

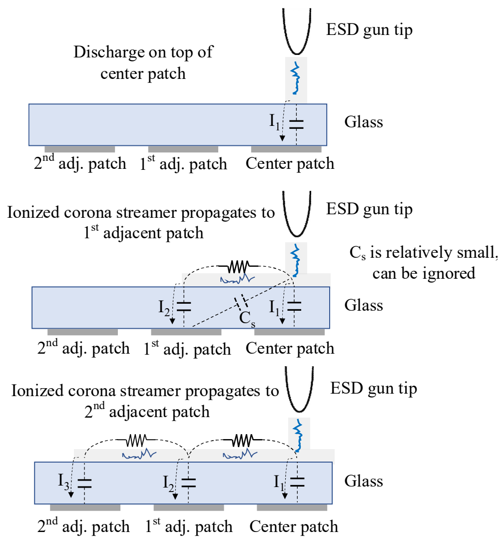

Fig. 2. Illustration of the corona discharge process on glass surface.

A setup similar to [2] was used to study the dust figures created by a corona discharge. An ESD gun was discharged to a glass surface with a mock touchscreen sensor patch array on the other side. After discharge, printer toner was blown on the glass surface. Fig. 3 shows an example of the resulting dust figure. The number of streamers observed in the dust figure provides a basis for geometric analysis of corona discharge modeling on the touchscreen surface.

III. Modeling of Corona Discharge and Coupling to Touchscreen Sensors

Fig. 3 indicates the geometry of the corona streamers flowing outward from the discharge location. These streamers can be statistically considered as evenly spaced in angle. Although a time- and charge- (current-) dependent model can more accurately capture the true behavior of streamer resistivity, here the resistivity is assumed to be quasi-static because the distance between patches is long enough that the resistivity of the most portion of the streamer becomes relative stable when it reaches the next patch. These assumptions set the basis to model the streamer source current and the effective resistance of the ionized air between sensor patches.

A. Streamer source current compensation

The dust figure in Fig. 3 shows that 6 out of 8 streamers over the discharge patch (i.e. center patch) continue out toward adjacent patches. The streamer current above the row and the column of the center patch is therefore modeled with a Current-Controlled-Current-Source (CCCS) as shown in Fig. 4 where 25% (i.e. 2/8) is lost when only considering the simplified current flow, and 75% (i.e. 6/8) of the ESD gun current is driven outward above the adjacent patches.

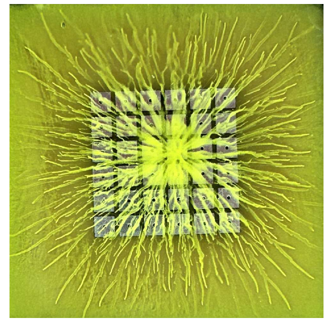

Fig. 3. Dust figure measurement on glass surface.

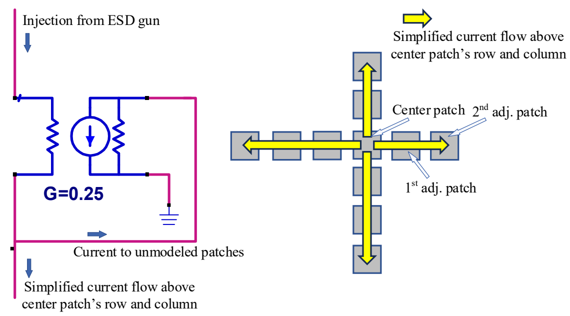

Fig. 4. Simplified geometry and compensation for current to unmodeled patches.

B. Effective resistance of ionized air

Since the streamers are roughly evenly spaced in angular distribution, the number of streamers that flow above a sensor patch can be captured with an arc above its leading edge, as shown in Fig. 5. As a result, the number of streamers flowing above the patch, n_1, is proportional to:

$$n_1 \propto \frac{l}{2\pi r} \tag{1}$$

where l denotes the arc length at the front edge of the first patch, and r denotes the distance from the discharge location to the arc of the front patch edge.

Consider each streamer as a single conductor and assume that each streamer will have the same per-unit-length resistance and that the resistivity of a single streamer is quasi-static. While this assumption is quite rough, it is acceptable as a first-order approximation. The resistance of a single streamer can then be calculated as:

$$R_{single} \propto \rho_{single} * r \tag{2}$$

where R_{single} denotes the resistance of a single streamer, and ρ_{single} denotes the per-unit-length streamer resistivity.

The total resistance from the area above center patch to the area above adjacent patches can be found from the resistance of n_1 streamers in parallel, which means:

$$R_1 = \frac{R_{single}}{n_1} = \frac{\rho_{single} * r}{n_{total} * \frac{l}{2\pi r}} \tag{3}$$

where R_1 denotes the resistance from the area above the center patch to the area above the first adjacent patch, and n_{total} denotes the total number of streamers on the glass leaving the discharge position.

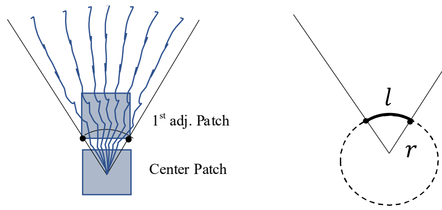

Fig. 5. Geometry of streamers propagating from the above area of center patch to the above area of first adjacent patch.

Because the patch size is fixed, the arc length l (shown in Fig. 5) remains almost the same, and the resistance from the area above center patch to the area above other patches changes with distance as:

$$R_1 \propto r^2 \tag{4}$$

While the total streamer resistance is proportional to r^2, the resistance between the above areas of other adjacent patches does not change as quickly. Assumption is made that the resistance from the area above center patch to the area above farthest patch is formed by the series resistance between the areas above adjacent patches. With such assumption, the proportionality between resistances is known, as shown in Fig. 6. As a result, models can be tuned using only R_1. This resistance can be used until the streamer propagation stops. At this point the streamer resistivity becomes very large (estimated to be 1 Mohm) because ionization stops and the voltage at the end of the streamer is clamped to a level low enough not to propagate (set to be 1.5 kV compared to 3 kV/mm air breakdown E-field).

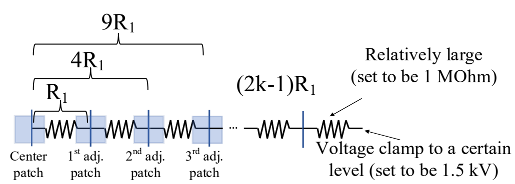

Fig. 6. Distribution of effective resistance ionized air on glass surface from the center patch outward.

C. SPICE model of corona discharge on touchscreen surface

In addition to the streamer source current compensation and effective streamer resistance, a SPICE model of corona discharge needs:

- An ESD gun model.
- A model of displacement current to a single patch circuitry or directly to return path.

An ESD gun model was used following the SPICE model shown in [18]. Displacement current to a single patch is modeled as shown in Fig. 7 [18]. A parasitic capacitance is added to R_{ITO}. A 50-ohm termination (either the oscilloscope's 50-ohm channel or the load termination) is in series with R_{ITO}. When the streamer propagation exceeds the patch matrix boundary, the current can still couple to the return path capacitively. The capacitance is considered to be glass capacitance in series with PCB to GND capacitance. The overall SPICE model of the corona discharge on a touchscreen surface is shown in Fig. 8 to model the current flow shown in Fig. 4. Only R_1 needs be optimized to fit measurements for different experimental conditions.

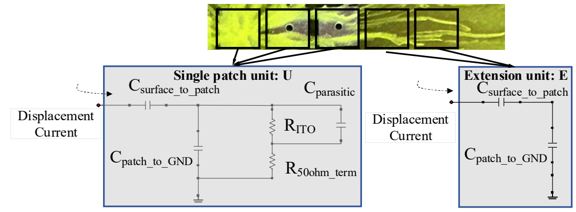

Fig. 7. SPICE model for coupling to a single patch unit (left) and the extension unit (right).

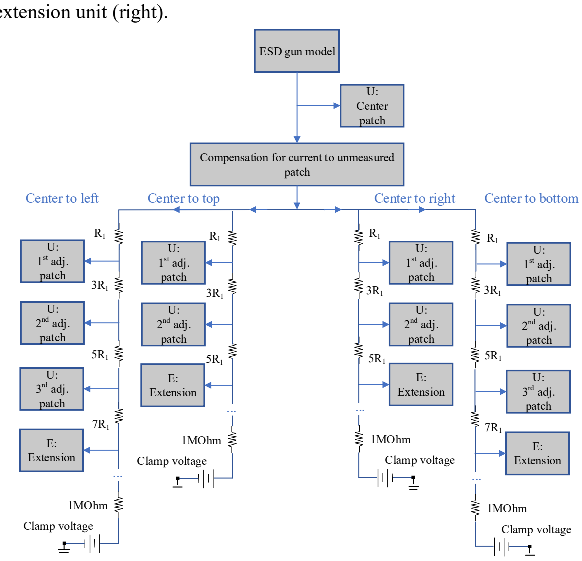

Fig. 8. SPICE model of corona discharge on a touchscreen surface.

IV. Results and Discussion

The value of R_1 was adjusted to match the ESD gun current between simulation and measurement, for multiple experimental setups with varying glass thickness, discharge voltage, and touch sensor circuitry. Fig. 9 and Fig. 10 show the results for two different thicknesses of glass, which correspond to 0.6 mm and 0.9 mm. The corresponding optimized value R_1 is 0.25 kOhm and 0.7 kOhm, respectively. The model shows that once ESD gun current can match, the overall peak current and charge for all patches are within 30% error.

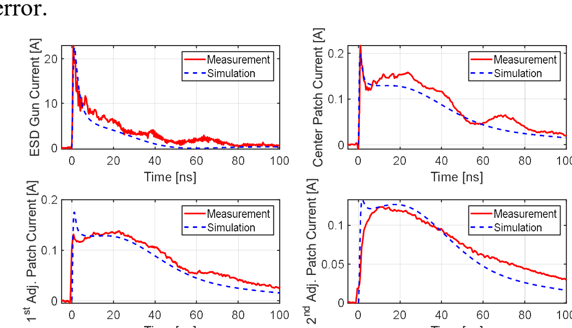

Fig. 9. C_{sp}=650 fF, C_{pg}=2.9 pF, R_{ITO}=10 kOhm at 15 kV discharge.

The optimized value of R_1 changes with the type and thickness of the glass, patch to ground capacitance, ITO resistance, and discharge voltage. Why and how R_1 changes with these factors (which digs deeper into how these factors affect the ionized air on glass) and how current on glass surface changes from above the adjacent patch to above the next patch are worth further study, but the current model can successfully predict the correlation between the ESD gun current and patch current. Unlike previous models, this model is built on physical observations in measured dust figures, and helps to explain why others saw improved modeling results when representing the corona surface discharge as a conductive disk whose resistance depended on radial distance from the discharge point.

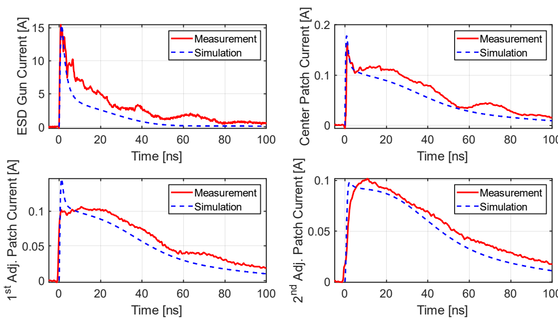

Fig. 10. C_{sp}=430 fF, C_{pg}=2.9 pF, R_{ITO}=10 kOhm at 15 kV discharge.

TABLE I. RESULTS WHEN CSP=650 FF

Current	Metric	Meas.	Sim.	Error
ESD Gun	Peak (A)	22.96	22.55	1.80%
	Charge (nC)	329.50	214.39	34.93%
	Rise time (ns)	0.44	0.60	36.36%
Center Patch	Peak (A)	0.22	0.20	8.49%
	Charge (nC)	8.59	7.18	16.39%
	Rise time (ns)	0.47	0.40	14.89%
1st adj. Patch	Peak (A)	0.14	0.18	27.02%
	Charge (nC)	8.17	7.16	12.35%
	Rise time (ns)	1.04	0.50	51.92%
2nd adj. Patch	Peak (A)	0.12	0.13	7.42%
	Charge (nC)	7.59	7.12	6.21%
	Rise time (ns)	6.39	0.80	87.48%

TABLE II. RESULTS WHEN CSP=430 FF

Current	Metric	Meas.	Sim.	Error
ESD Gun	Peak (A)	15.44	15.40	0.26%
	Charge (nC)	289.80	147.22	49.20%
	Rise time (ns)	0.45	0.60	33.33%
Center Patch	Peak (A)	0.16	0.18	9.03%
	Charge (nC)	6.37	5.01	21.36%
	Rise time (ns)	0.49	0.40	18.37%
1st adj. Patch	Peak (A)	0.11	0.14	27.27%
	Charge (nC)	6.07	4.99	17.81%
	Rise time (ns)	1.21	0.50	58.68%
2nd adj. Patch	Peak (A)	0.10	0.10	3.46%
	Charge (nC)	5.62	4.93	12.24%
	Rise time (ns)	5.61	1.10	80.39%

V. CONCLUSION

A new methodology for modeling corona discharge to a touchscreen surface is proposed. The model assumes an equivalent resistance of ionized air above the patches, which is derived from observations of experimental dust figures. The only parameter that must be optimized to fit measured and modeled results is the effective streamer resistance between the area above the discharge patch and the area above the first adjacent patch. The error between the measured and modeled patch peak current and charge is less than 30%. Further work is needed to incorporate the change in the effective streamer resistance over time and to predict it with parameters like the discharge voltage, the characteristics of glass, and sensor circuitry.

REFERENCES

[1] Y. Gan et al., "Experimental Characterization and Modeling of Surface Discharging for an Electrostatic Discharge (ESD) to an LCD Display," in *IEEE Transactions on Electromagnetic Compatibility*, vol. 60, no. 1, pp. 96-106, Feb. 2018.

[2] Z. Peng et al., "Trend Analysis of Dissipated Electrostatic Discharge Energy in Touchscreen Displays," *2020 IEEE International Symposium on Electromagnetic Compatibility & Signal/Power Integrity (EMCSI)*, Reno, NV, USA, 2020, pp. 188-193.

[3] Z. Peng et al., "Characterization and Modeling of Commercial ICs for System-Efficient ESD Design," in *IEEE Transactions on Electromagnetic Compatibility*, vol. 64, no. 6, pp. 1802-1811, Dec. 2022.

[4] Electromagnetic compatibility (EMC) - Part 4-2: Testing and measurement techniques - Electrostatic discharge immunity test, IEC International Standard, 61000-4-2, 2008.

[5] A. Norberg, "Modeling current pulse shape and energy in surface discharges," in *IEEE Transactions on Industry Applications*, vol. 28, no. 3, pp. 498-503, May-June 1992.

[6] E. Marode, "The mechanism of spark breakdown in air at atmospheric pressure between a positive point and a plane. I. Experimental: Nature of the streamer track," *Journal of Applied Physics*, vol. 46, no. 5, pp. 2005–2015, May 1975.

[7] X. Wen, X. Yuan, L. Lan, M. Long and L. Hao, "Study on the Effective Ionization Rate of Atmospheric Corona Discharge Plasmas by Considering Humidity," in *IEEE Transactions on Plasma Science*, vol. 44, no. 12, pp. 3386-3391, Dec. 2016.

[8] A. Talebzadeh, Y. Gan, K. -H. Kim, Y. Zhang and D. Pommerenke, "Spark-less electrostatic discharge (ESD) on display screens," *2015 IEEE International Symposium on Electromagnetic Compatibility (EMC)*, Dresden, Germany, 2015, pp. 1284-1289.

[9] S. Shinde et al., "ESD to the display inducing currents measured using a substitution PC board," *2016 IEEE International Symposium on Electromagnetic Compatibility (EMC)*, Ottawa, ON, Canada, 2016, pp. 707-712.

[10] H. Rezaei et al., "Experimental characterization and methodology for full-wave modeling of ESD to displays," *2020 IEEE International Symposium on Electromagnetic Compatibility & Signal/Power Integrity (EMCSI)*, Reno, NV, USA, 2020, pp. 182-187.

[11] G. C. Lichtenberg, *De Nova Methodo Naturam Ac Motum Fluidi Electrici Investigandi*, Commentarii Societatis Göttingen, 1778.

[12] C. Li et al., "Dust Figures as a Way for Mapping Surface Charge Distribution — A Review," in *IEEE Transactions on Dielectrics and Electrical Insulation*, vol. 28, no. 3, pp. 853-863, June 2021.

[13] Yuzo Takahashi, "Two hundred years of lichtenberg figures," *Journal of Electrostatics*, vol. 6, no. 1, pp. 1-13, 1979.

[14] P. O. Pedersen, "Part I. A Preliminary Investigation," in *On The Lichtenberg Figures*, Bianco Lunos Bogtrykkeri, Copenhagen, Denmark, 1919.

[15] Y. Murooka, and S. Koyama, "Nanosecond surface discharge study by using dust figure techniques." *Journal of Applied Physics*, vol. 44, no. 4, pp. 1576-1580, 1973.

[16] Y. Murooka, T. Takada and K. Hiddaka, "Nanosecond surface discharge and charge density evaluation Part I: review and experiments," in *IEEE Electrical Insulation Magazine*, vol. 17, no. 2, pp. 6-16, March-April 2001.

[17] Z. Shi, C. Li, Z. Lei, Y. Yang, J. He and J. Song, "Lichtenberg figures presenting electrostatic discharge patterns at different humidity," *Journal of Physics D: Applied Physics*, vol. 54, 2021.

[18] J. Zhou, C. W. Lam, Z. Peng, D. Beetner and D. Pommerenke, "Characterization and Modeling of Sparkless Discharge to a Touch Screen Display," *2023 IEEE Symposium on Electromagnetic Compatibility & Signal/Power Integrity (EMC+SIPI)*, Grand Rapids, MI, USA, 2023, pp. 510-515.

[19] J. M. Meek and J. D. Craggs, Electrical breakdown of Gases, Wiley, New York, 1978.